Available online at www.sciencedirect.com
SCIENCE DIRECT
Tectonophysics 422 (2006) 115–128
TECTONOPHYSICS
www.elsevier.com/locate/tecto

Mesozoic thermal history of the Prebetic continental margin (southern Spain): Constraints from apatite fission-track analysis

L. Barbero [a,*], A.C. López-Garrido [b]

[a] Departamento de Geología, Facultad de CC del Mar y Ambientales, Universidad de Cádiz, Campus de Puerto Real, 11510 Puerto Real (Cádiz), Spain
[b] Instituto Andaluz de Ciencias de la Tierra, CSIC-Universidad de Granada, Facultad de Ciencias, Avd[a] Fuentenueva s/n, 18071 Granada, Spain

Received 3 November 2005; received in revised form 9 May 2006; accepted 12 May 2006
Available online 7 July 2006

Abstract

Apatite fission-track analysis was applied to Triassic and Cretaceous sediments from the South-Iberian Continental Margin to unravel its thermal history. Apatite fission-track age populations from Triassic samples indicate partial annealing and point to a maximum temperature of around 100–110 °C during their post-depositional evolution. In certain apatites from Cretaceous samples, two different fission-track age populations of 93–99 and around 180 Ma can be distinguished. Track lengths associated with these two populations enabled thermal modelling based on experimental annealing and mathematical algorithms. These thermal models indicate that the post-depositional thermal evolution attained temperatures ≤ 70 °C, which is consistent with available vitrinite-reflectance data. Thermal modelling for the Cretaceous samples makes it possible to decipher a succession of cooling and heating periods, consisting of (a) a late Carboniferous–Permian cooling followed by (b) a progressive heating episode that ended approximately 120 Ma at a maximum *T* of around 110 °C. The first cooling episode resulted from a combination of factors such as: the relaxation of the thermal anomaly related to the termination of the Hercynian cycle; the progressive exhumation of the Hercynian basement and the thermal subsidence related to the rifting of the Bay of Biscay, reactivated during the Late Permian. Jurassic thermal evolution deduced from the inherited thermal signal in the Cretaceous sediments is characterized by progressive heating that ended around 120 Ma. This heating episode is related to thermal subsidence during Jurassic rifting, in agreement with the presence of abundant mantle-derived tholeiitic magmas interbedded in the Jurassic rocks. The end of the Jurassic rifting is well marked by a cooling episode apparently starting during Neocomiam times and ending at surface conditions by Albian times.
© 2006 Elsevier B.V. All rights reserved.

Keywords: Apatite fission tracks; Thermochronology; Rifting; Subsidence; Betic Cordilleras

1. Introduction

The Betic Cordillera, located in south-eastern Spain, is part of the Perimediterranean Alpine orogen. This orogen comprises the Betic and Rif cordilleras, which lie north and south of the Alborán basin in the westernmost Mediterranean sea. Both cordilleras form an arc-shaped orogen which joins across the Gibraltar strait. Three main tectonic units have been distinguished in the Betic cordillera, (Vera and Martín-Algarra, 2004): a) the first unit, known as External zones, represents the pre-Miocene palaeomargin to the south of the Iberian plate; b) the second tectonic unit, called the Internal zones, forms the most deformed part of

* Corresponding author.
E-mail address: luis.barbero@uca.es (L. Barbero).

0040-1951/$ - see front matter © 2006 Elsevier B.V. All rights reserved.
doi:10.1016/j.tecto.2006.05.011

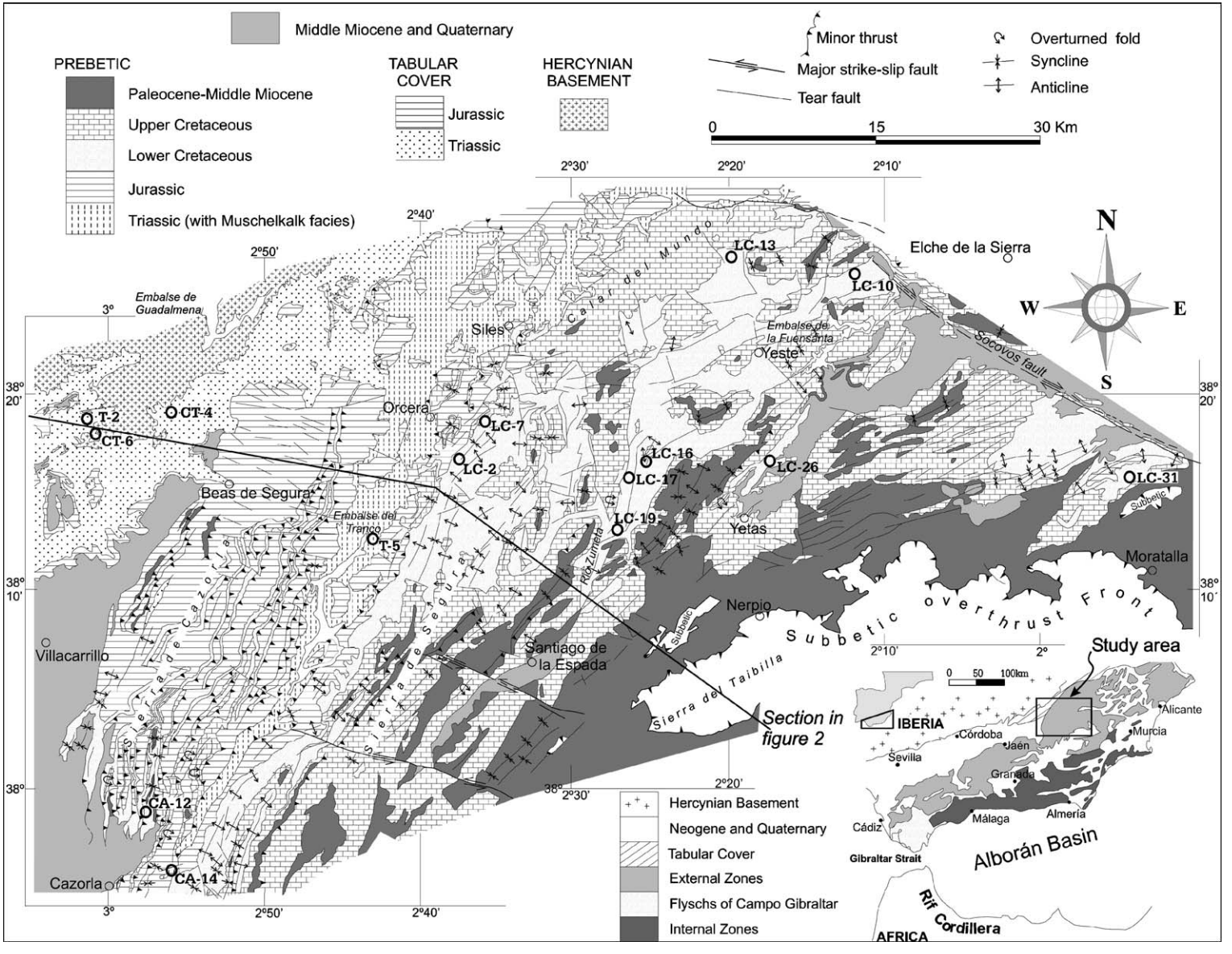

Fig. 1. Geological map of the study area (modified and completed after García-Hernández et al., 2004) with the location of samples. Insets show the location of the area on the Iberian Peninsula in the context of the entire Betic cordilleras.

the orogen and is comprised essentially of several variably metamorphosed nappe complexes; c) the Campo de Gibraltar Complex, which outcrops between the Internal and External Betic zones, extending widely throughout the provinces of Cadiz and Malaga. Their sediments, from the Cretaceous to the Lower Miocene, are deposited in a deep-water flysch basin (Fig. 1).

The stratigraphy, palaeogeography and tectonosedimentary processes in the Betic margin have been extensively studied during the last two decades. Reviews on the main aspects of the Betic margin can be found in Vera (2001) and Martín-Chivelet et al. (2002) and references therein. Hanne et al. (2003) have recently analysed the subsidence throughout the entire Betic cordillera. Nevertheless, certain aspects concerning the geological history of the Prebetic margin, such as the thermal evolution from Mesozoic to present, were considered for the first time only recently (Barbero et al., 2001). Here we provide an example from the External zones of the Betic cordillera concerning how low-temperature thermal histories of source areas can be reconstructed using the information contained in detrital products trapped in the marginal basins.

Fission-track studies are used to unravel the cooling histories of the different parts of an orogen (Gallagher, 1995; Gallagher and Brown, 1997; Gallagher et al., 1998). Cooling may reflect either erosional or tectonic exhumation processes or both. The fission-track age of a detrital mineral is the result of the duration of cooling through the partial-annealing zone (temperature interval in which fission-track lengths are reduced or annealed), transport, and any post-depositional thermal history (Lonergan and Johnson, 1998). In the case of detrital minerals which bring a thermal history recorded in the fission-track length distribution and associated age, if transport (lag time as defined by Garver and Brandon, 1994) is considered instantaneous, and post-depositional annealing is weak or negligible, the thermal history of the sources could be reconstructed. In most inverted sedimentary basins, the most recent tectonic event which led to the exhumation of the basin is the only process recorded in the apatite fission-track system, in which any other previous thermal history is generally overprinted.

The present work provides new apatite fission-track data from the Prebetic Triassic and Cretaceous sediments of the Sierra de Cazorla–Sierra de Segura region with the aim of establishing a thermal evolution history consistent with the available stratigraphic, tectono-sedimentological and subsidence data for Mesozoic times, in an area with a nearly complete lack of other thermal indicators.

2. Geological setting

In the Betic Cordilleras, a tectonosedimentary division between External and Internal zones has traditionally been made (Fig. 1). The allochthonous Palaeozoic basement and Triassic to Cenozoic cover materials constitute the Internal zone, which shows a complex nappe structure and a variable degree of metamorphism. Allochthonous units of the Internal zones belong to the so-called Alborán Domain, a crustal unit separated by oceanic crust from Iberia and

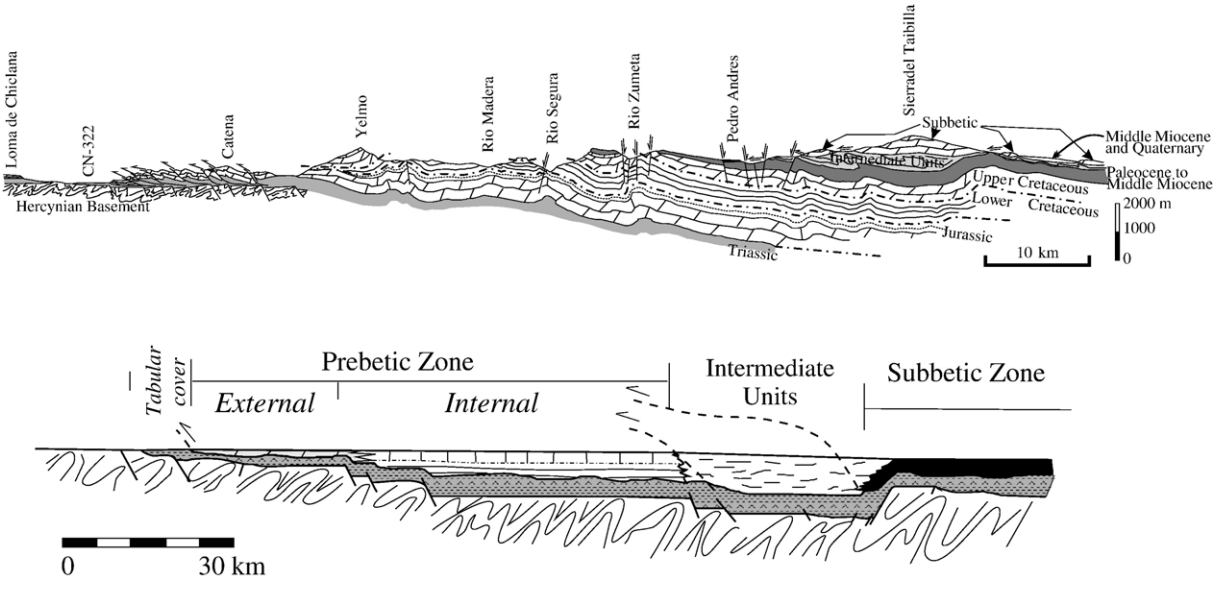

Fig. 2. Geological section across the External zone (above) and restored cross section (below) modified after García-Hernández et al. (1980) and Vera (2001). Location of the section is marked in Fig. 1.

Africa during Jurassic to Palaeogene times. Sedimentary deposits, accumulated in the continental margin of the Iberian plate during the Mesozoic to Tertiary constitute the External zones of the Betic Cordilleras. The External zones are further subdivided into two different domains based on tectonosedimentary criteria: the Prebetic and the Subbetic zone. The Prebetic zone, composed mainly of shallow marine deposits with intercalations of continental terrigenous sediments, constitutes the autochthonous terrane relative to the Subbetic zone that overthrusts it (García-Hernández et al., 1973, 1980). The structure of the External Zones consists of a series of thin-skinned nappes comprising Triassic to Middle Miocene sedimentary sequences which are detached from their Palaeozoic substratum, the Triassic sediments acting as detachment level. For the Prebetic zone, there is a major shortening of the cover, especially in the External Prebetic (Sierra de Cazorla), which has an imbricated thrust-fault structure also with narrow westward verging overturned folds. In this area the shortening is estimated to be a minimum 15 km (Dabrio and López-Garrido, 1970). The Internal Prebetic shows a gentler fold-and-fault structure (Fig. 2). The overall structure of the External Zones formed in response to the westward drift of the so-called Alborán Domain and its collision with the Southern Iberian Continental Margin (SICM) (Sanz de Galdeano, 1990; Vera, 2001).

The Prebetic zone, where the present work is based, is traditionally subdivided on the basis of stratigraphic and tectonic criteria, into two areas: the External Prebetic and the Internal Prebetic. The External Prebetic, the area closest to the Hercynian basement, is characterized by frequent stratigraphic gaps, a scarcity of Portlandian to Lower Valanginien sediments, and extensively exposed Liassic and Dogger sediments.

The Internal Prebetic, located basinwards, has progressively thicker sequences towards the SE, with a thick sequence of Upper Jurassic and Lower Cretaceous sediments. These represent the more distal areas with respect to the External Prebetic and form a transition into the deep marine environments characteristic of the more internal Subbetic Zone.

Between the Prebetic zone and the Hercynian basement, the Tabular Cover crops out, with non-deformed sediments (Figs. 1 and 2). Triassic red beds (mudstones and sandstones) of the Tabular Cover unconformably overlie the Palaeozoic basement. The Prebetic succession of Ladinian–Carnian age (Gil et al., 1987) is composed mainly of alternating red mudstones and red sandstones with scarce thin carbonate beds (Muschelkalk facies). Despite strong lateral variation in the facies, the average thickness is about 315 m. Lateral continuity exists between the Triassic series of the Tabular Cover and those of the Prebetic, the series thickening basinwards and showing an increased number of intercalated carbonate beds of Muschelkalk facies. Lower Cretaceous terrigenous sediments are of Barremian, Aptian and Albian age and rest disconformably on different Jurassic carbonate formations and on Prebetic Triassic sediments in the Siles region (Fig. 1). These terrigenous facies, which are hectometric beds within widespread carbonates, formed in shallow-water environments. The total thicknesses of these deposits are of up to 3000 m. Terrigenous materials, especially those of the Utrillas formation (Albian) are extensively exposed.

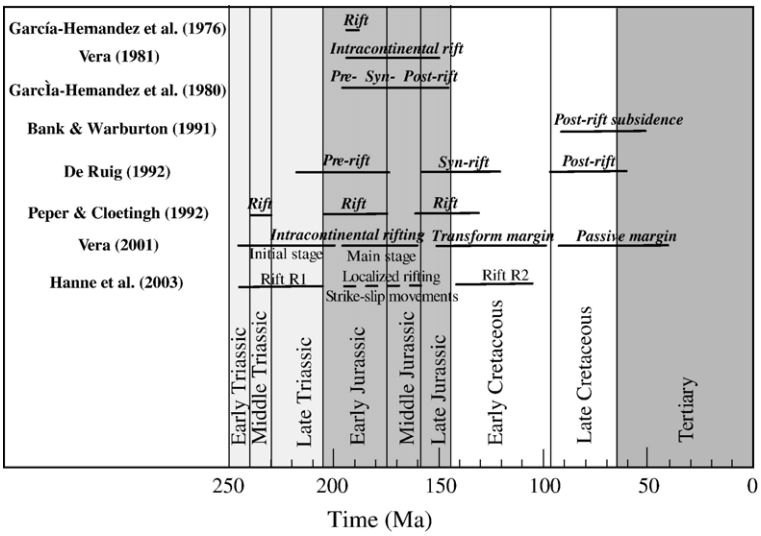

Fig. 3. Summary of the different models on the evolution of the Betic continental margin.

Different authors have studied the evolution of the SICM, the main proposals being summarized in Fig. 3. García-Hernández et al. (1976, 1980) and Vera (1981) proposed a unique rifting stage during Jurassic times, while Banks and Warburton (1991) were the first authors to suggest that the Upper Cretaceous to Lower Tertiary sediments were deposited during a post-rift subsidence stage. De Ruig (1992) considered a single rifting event to be marked by Pre-, Syn-, and Post-rift phases occurring during Triassic–Middle-Jurassic, Late Jurassic–Early Cretaceous and Late Cretaceous, respectively. Peper and Cloetingh (1992) proposed that the evolution of the SICM spanned three different rifting stages (Mid-Triassic, Early Jurassic, and Late Jurassic–Early Cretaceous). In more recent models (e.g. Vera, 2001), the evolution of the Betic Margin is also presented in four different stages: 1) A Triassic intracontinental rifting stage is related to the opening of the Tethys ocean and to the dismembering of the Pangea supercontinent (Pérez-López, 1991). The geometry of the Triassic basin related to this rifting stage has been obliterated by later events (Vilas et al., 2001). 2) A post-rifting stage (transform margin stage) is characterized by the development of carbonate platforms during the Lower to Middle Jurassic. Simultaneously, the opening of the South Atlantic Ocean started (Vera, 1988), creating the accommodation space necessary for the deposition of the Subbetic sediments. 3) During the Late Jurassic to Middle Cretaceous rifting stage related to the opening of the North Atlantic Ocean, an extensional episode is recognized in the Betic margin (Arias et al., 1996). During this stage, the Prebetic domain was separated from the rest of the Betic basin and also from the rest of the Iberian Plate (Vilas et al., 2001). 4) A post-extensional stage (passive margin stage) began during the Albian. This post-extensional stage continued during the Upper Cretaceous, when the African approached the Iberian plate. The destruction of the Prebetic margin due to the collision with the African and Iberian plates started in Palaeogene times, the main collision event occurring in the Miocene (Vegas and Banda, 1982). Hanne et al. (2003) made an integrated study of the results of subsidence analysis using standard backstripping techniques across and along the entire orogen. They modelled the data by using a strain-rate inversion technique (White, 1993) to determine the number, duration and intensity of the rifting events. Three phases of rapid subsidence interpreted as rifting stages during Permo-Triassic, Late Triassic to Early Jurassic, and Late Jurassic to Early Cretaceous were recognized (Hanne et al., 2003).

Data on the thermal history of the SICM are very scarce. Lonergan and Johnson (1998), using fission-track detrital thermochronology reconstructed the cooling and unroofing history of the sedimentary source areas during the Oligocene–Miocene in a synorogenic foreland basin located in the Internal zone of the Betic cordillera. Stapel (1999) made an apatite fission-track profile in Hercynian basement rocks from the Algarve (south-western Portugal) to Sierra Morena (southern Spain; see Fig. 7) in an attempt to relate the different geophysical characteristics of the West and Central Iberian Regions to the cooling history. This author perceived a strong difference between the west and central Iberian regions in terms of fission-track ages, thus suggesting different cooling histories. For the Central Iberian Region, fission-track data point to a slow cooling through the partial-annealing zone while, for the West Iberian Region, data are compatible with strong cooling events at ~112 and 60 Ma. In a preliminary fission-track study in the same area of the present work, Barbero et al. (2001) contended that vitrinite reflectance Ro% values from Albian sandstones taken in the Socovos-2 borehole (located close to the NW of the study area) are below Ro=0.5%, implying maximum temperatures of probably lower than 70–80 °C during the post-depositional evolution.

The study area selected for the present work (the Tabular Cover, and the Sierra de Cazorla and Sierra de Segura in the Prebetic) is located between the Guadalquivir foreland basin to the northwest and the Subbetic overthrust front located to the southeast (Fig. 1). The Hercynian basement constitutes the north-western limit. Toward the northeast, the Socovos strike-slip fault zone separates the study area from another part of the Prebetic, the Albacete Domain, which was a slowly subsiding area during the Cretaceous and marks the transition between the Hercynian basement and the more subsiding areas of the rest of the External Betic zones (Martín-Chivelet et al., 2002).

For the present study, samples were collected from: 1) Triassic red sandstones, both from the Tabular Cover and from the Prebetic; 2) Lower Cretaceous sands. Heavy minerals recovered in these sediments include, in order of decreasing abundance, tourmaline, garnet, zircon, apatite, rutile, opaque minerals, and sillimanite. Jurassic materials in the area are carbonates and it is not possible to sample any terrigenous sediments of this age.

3. Fission-track methodology

Spontaneous fission of ^{238}U creates tracks that, once properly etched, can be counted and measured under an optical microscope. With the ζ approach (Hurford and Green, 1983) and the external detector method, fission track ages of individual apatite crystals can be determined. Fission tracks are shortened during heating at a rate dependent mainly on the temperature and composition in

Table 1
Apatite fission track age data of samples from the Sierra de Segura and Sierra de Cazorla

Sample no.	Stratigraphic age	No. of grains	CN-5 track density ($\times 10^6$ tr/cm^2) (*no. of tracks*)	Spontaneous track density ($\times 10^6$ tr/cm^2) (*no. of tracks*)	Induced track density ($\times 10^6$ tr/cm^2) (*no. of tracks*)	Central age $\pm 1\sigma$ (Ma) $P(\chi^2)$	Age populations (Ma$\pm 1\sigma$), N_f, W (%)				Fit statistics
							P1	P2	P3	P4	
T-2	Triassic	20	1.011 (*4691*)	2.386 (*1261*)	1.830 (*967*)	231±23. *0.00*		189±9 N_f=16 W=22		518± 67 N_f=4 W=29	χ^2=19, l=17 $P(F)$=0%
T-5	Triassic	23	1.024 (*4754*)	3.175 (*2099*)	3.160 (*2092*)	173±15 *0.00*	108±6. N_f=7.8 W=18		216±10 N_f=15.2 W=17		χ^2=25, l=20 $P(F)$=0%
LC-2	Aptian	32	1.097 (*5087*)	4.479 (*3424*)	4.146 (*3169*)	186±12 *0.00*	89±10 N_f=3.4 W=22	158±9 N_f=11.7 W=18	239±10 N_f=16.9 W=15		χ^2=29, l=27 $P(F)$=0%
LC-7	Aptian	19	1.034 (*4791*)	4.168 (*3343*)	3.273 (*2625*)	215±14 *0.00*		141±11 N_f=4.1 W=15	241±9 N_f=14.9 W=13		χ^2=21, l=16 $P(F)$=0%
LC-2+ LC-7	Aptian	51	–	4.320 (*6767*)	3.800 (*5794*)	197±9 *0.00*	87±10 N_f=3 W=22	154±9 N_f=17.3 W=17	241±8 N_f=30.7 W=17		χ^2=49, l=46 $P(F)$=0%
LC-13	Albian	22	0.982 (*4555*)	3.797 (*2862*)	3.231 (*2436*)	200±15 *0.00*	116±10 N_f=3.1 W=14	200±8 N_f=16.8 W=15		456±84 N_f=2.1 W=21	χ^2=22, l=17 $P(F)$=1%
LC-10	Aptian	26	1.008 (*4673*)	4.103 (*2998*)	4.330 (*3164*)	157±11 *0.00*	97±6 N_f=7.2 W=17	188±7 N_f=18.8 W=15			χ^2=26, l=23 $P(F)$=0%
LC-13+ LC-10	Aptian	48	–	3.950 (*5860*)	3.720 (*5600*)	176±9 *0.00*	102±6 N_f=10 W=16	193±6 N_f=35.9 W=16		457±80 N_f=2.1 W=21	χ^2=50, l=43 $P(F)$=0%
LC-31	Albian	33	0.997 (*4628*)	3.335 (*5239*)	3.639 (*5715*)	142±9 *0.00*	99±3 N_f=15.3 W=13	188±6 N_f=17.7 W=13			χ^2=33, l=30 $P(F)$=0%
LC-26	Barrem	11	0.983 (*4566*)	3.71 (*1204*)	3.323 (*1024*)	175±8 *44.91*					
LC-17	Albian	17	0.944 (*4378*)	3.109 (*1616*)	2.999 (*1752*)	153±13 *0.00*	96±10 N_f=4.4 W=18	177±8 N_f=12.6 W=16			χ^2=20, l=14 $P(F)$=0%
LC-16	Albian	8	0.957 (*4437*)	4.300 (*1274*)	3.936 (*1166*)	162±17 *0.00*					
LC-17+ LC-16	Albian	25	–	3.510 (*2890*)	3.310 (*2918*)	156±10 *0.00*	103±7 N_f=7.1 W=14	181±7 N_f=17.9 W=15			χ^2=30, l=22 $P(F)$=0%
LC-19	Albian	37	0.918 (*4259*)	3.970 (*9028*)	4.010 (*9111*)	140±9 *0.00*	93±3 N_f=14.8 W=14	175±5 N_f=22.2 W=9			χ^2=44, l=34 $P(F)$=0%

Ages determined by EDM method using a zeta value (LB) of 337.8±5.2 for dosimeter CN-5.

N_f number of grains in age population; W relative standard deviation; χ^2 goodness of fit parameter; l degrees of freedom; $P(F)$ probability that the random variation alone could produce the observed F value for peak 2 or 3.

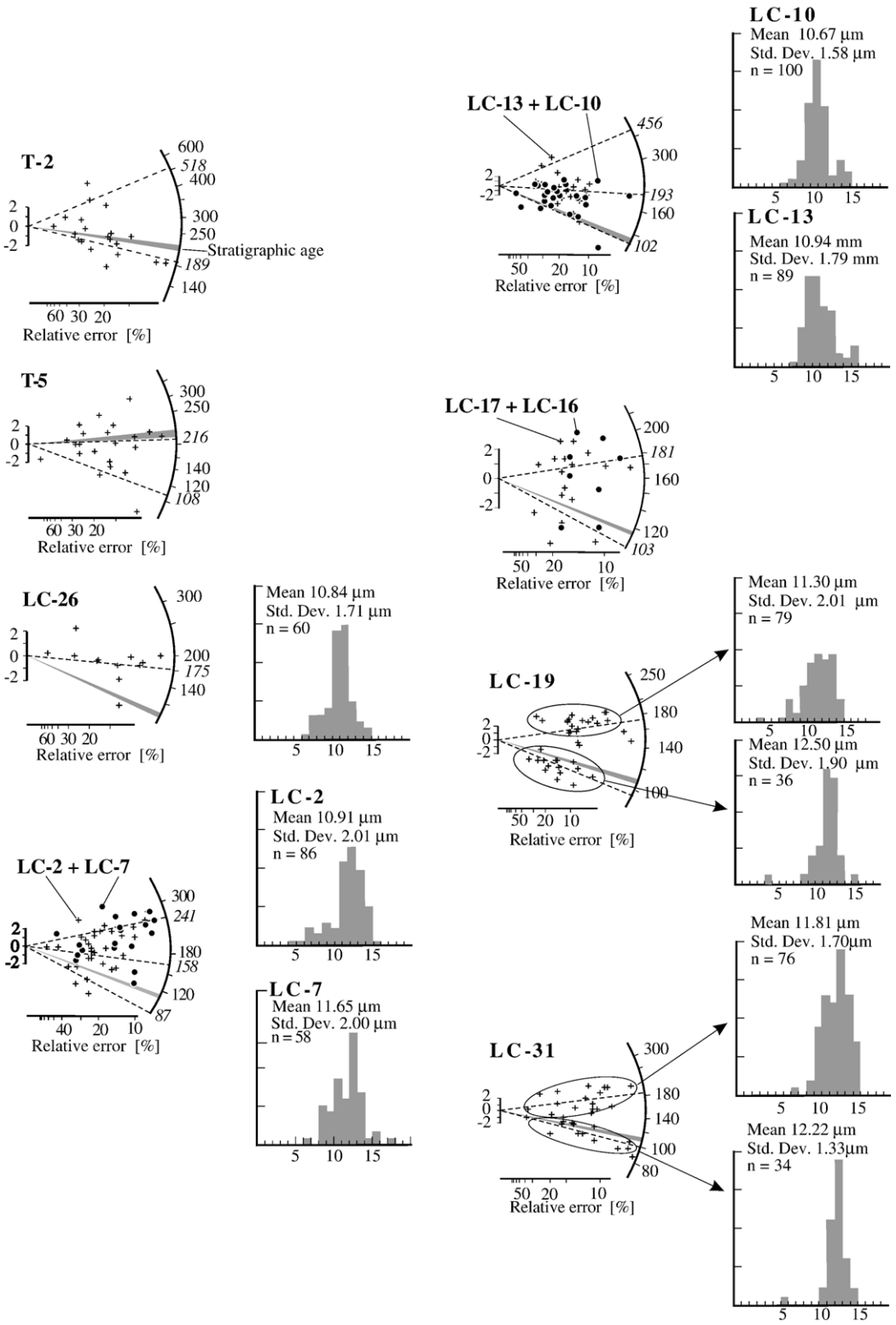

Fig. 4. Radial plots and track-length histograms for apatites recovered in Triassic and Cretaceous sediments from the Betic continental margin. For location of samples, see Fig. 1.

terms of F and Cl contents in apatite, Cl apatites being more resistant to annealing than F apatites. The result of this annealing process is that in apatite, the initial length of 15–17 μm is shortened if the heating temperature is in the range of 60–120 °C over geological timescales. For this reason, the cooling–heating pattern followed by a particular sample, will result in a particular track-length distribution and associated apatite fission-track age. Fast cooling through the partial-annealing zone (PAZ) will result in narrow track-length distributions with track lengths > 14 μm. More complex thermal histories involving several cooling–heating events or slow cooling through the PAZ will result in broader track-length distributions. The use of experimental annealing results on apatites from different compositions and inverse modelling via Monte Carlo and genetic algorithms simulations (Gallagher, 1995; Ketcham et al., 2000) provide a thermal history that agrees with the track-length distribution and the fission-track age. The success in finding a consistent thermal history by modelling can be highly dependent on the appropriate use of the known geological constraints imposed on the models. Apatites were extracted from sediments and sedimentary rocks by crushing, sieving, and using standard heavy-liquid as well as magnetic-separation techniques.

Apatites were mounted in U-free glass with clear epoxy resin and polished. Etching to reveal fossil tracks was performed using 5 M HNO_3, at 20 ± 0.5 °C for 20 s. The external-detector method was used, the detector being a U-free clear ruby muscovite. After the detector was placed, the samples were sent to the HIFAR reactor (Australia) for irradiation with thermal neutrons. The ζ approach (Hurford and Green, 1983) was used for fission-track analysis of individual apatite crystals.

Counting was performed using a Zeiss Axioskop 2 microscope (100× oil lens, 1250× total magnification) equipped with a Kinetek automated stage. Ages were calculated using the TRACKKEY program, following Dunkl (2001). The track-length measurements were made using a drawing tube linked to a computer-controlled digital tablet with a tiny red LED in the cursor. Reported D_{par} (the length of the track pits etched parallel to the crystallographic *c*-axis) values, are the result of averaging 200 measurements. The tablet was calibrated by repeated measurements ($n = 50$) made using a 100-μm graticule with 2-μm divisions.

In sedimentary samples, the fission-track data gathered can be very complex due either to the presence of different sources exhumed at different times and/or to the presence of apatites with different Cl and F contents which anneal at different rates. This could result in the presence of several age components. The best fit binomial peak-fitting routine of Galbraith and Green (1990) was used to deconvolve the fission-track grain-age spectra in samples containing more that one age population. Calculations were performed using the Windows version of the BINOMFIT program of Brandon (1992, 1996). The procedure is based on the maximum-likelihood method, where the best-fit solution is determined by comparing the age distribution of the data to a predicted mixed binomial distribution. The significance of the number of resulting age peaks was assessed with the *F* test. When, for a given number of peaks (n), F was large, the improvement of the fit associated with an additional peak was considered significant, and the calculation was repeated using $n+1$ peaks and so on.

In apatites, the commonly low amount of U leads to relatively low spontaneous track densities, and the deconvolution of peaks requires a large number of crystals to be measured. This problem was minimized, in the present work, by amalgamating the samples from the same stratigraphic level and those from nearby localities. Results from both amalgamated and non-amalgamated samples are shown in Table 1.

Cl and F compositions were measured at Universidad Complutense de Madrid by electron microprobe (JEOL Superprobe JXA 8900-M) operated at 15 kV and a beam current of 20 nA in spots of 10 μm in diameter. About 2 min was necessary for each spot analysis.

4. Apatite fission-track results

Analytical data are listed in Table 1 and the locations of samples are marked in Fig. 1. The radial plots of eight samples corresponding to the sands of Barremian–Aptian–Albian depositional age, one Triassic red sandstone from the Tabular Cover (T-2) and another from the External–Internal Prebetic limit (T-5) are shown in Fig. 4. The Triassic sample T-2 has a population of apatite grains younger (189 Ma) than the depositional age (Carnian, around 215 Ma), and a population much older with grains older than 400 Ma. In the other Triassic sample, T-5, two populations can be distinguished (108 and 216 Ma), with at least one of the ages clearly younger than the depositional age (Carnian, around 215 Ma).

In the Cretaceous samples LC-7, LC-13, LC-2, LC-17, LC-19 and LC-31 almost all individual apatite fission-track ages are older than the stratigraphic depositional age (Aptian–Albian). In sample LC-2 and in the amalgamated sample LC-2 + LC-7, a population younger than depositional age is recognised, despite that it contains only 3 grains. Mean track lengths in individual samples are 10.91 and 11.65 μm, and indicate partial annealing. In samples LC-19 and LC-31, the southernmost and easternmost

samples, respectively, two populations can be clearly distinguished: the first one of 175–188 Ma, which is older than the depositional age, and a second population of 93–99 Ma which postdates deposition. Track lengths were measured separately in these two populations in sample LC-19 and LC-31. In both cases, lengths associated with the older population had an average of 11.3 and 11.8 μm with standard deviations of 2.01 and 1.70, respectively, the histograms being negatively skewed. In the younger population, average track lengths were 12.5 and 12.2 μm with standard deviations of 1.9 and 1.33. The D_{par} were measured in the two age components of samples LC-19 and LC-31, the mean values being 1.36 and 1.33 μm, respectively. Fig. 5 presents the D_{par} versus age data in the two populations. No correlation between D_{par} and age was found in any case. The F and Cl contents were measured in three samples (Fig. 5). All apatite measured was fluorapatite with an averaged Cl content of 0.07 (% wt). No differences were detected between samples or between the young and old populations in samples LC-19 and LC-31.

5. Thermal modelling

Apatite fission track ages from terrigenous sediments can record different histories: the post-depositional thermal history recorded in fission tracks is better resolved in cases where maximum post-depositional temperatures were high enough to completely anneal the fission tracks. The thermal history of the source areas is recorded in cases where the post-depositional thermal history failed to reach temperatures of the partial-annealing zone. In cases that, during the post-depositional evolution of the basin, reached temperatures within the partial-annealing zone, thermal modelling is hampered by the fact that the inherited thermal signal is partially reset during the post-depositional history, making any thermal modelling of the source area uncertain. Nevertheless, when the source area is exhumed rapidly because of high temperatures, a fairly accurate post-depositional history can be model as the fission-track grain ages and lengths are only slightly changed by the short inherited thermal history.

An additional problem when performing fission-track thermal modelling is related to the presence of different age populations in a single sedimentary sample. Usually it is not easy to establish a representative number of horizontally confined fission-track lengths for each population, thus making modelling impossible. In our case, in selected samples from Albian sediments, we assigned track lengths to each of the two populations. This is the case of samples LC-19 and LC-31, which were then selected for thermal modelling. For this purpose, Laslett et al. (1987) annealing models were used, as Cl contents of the samples were

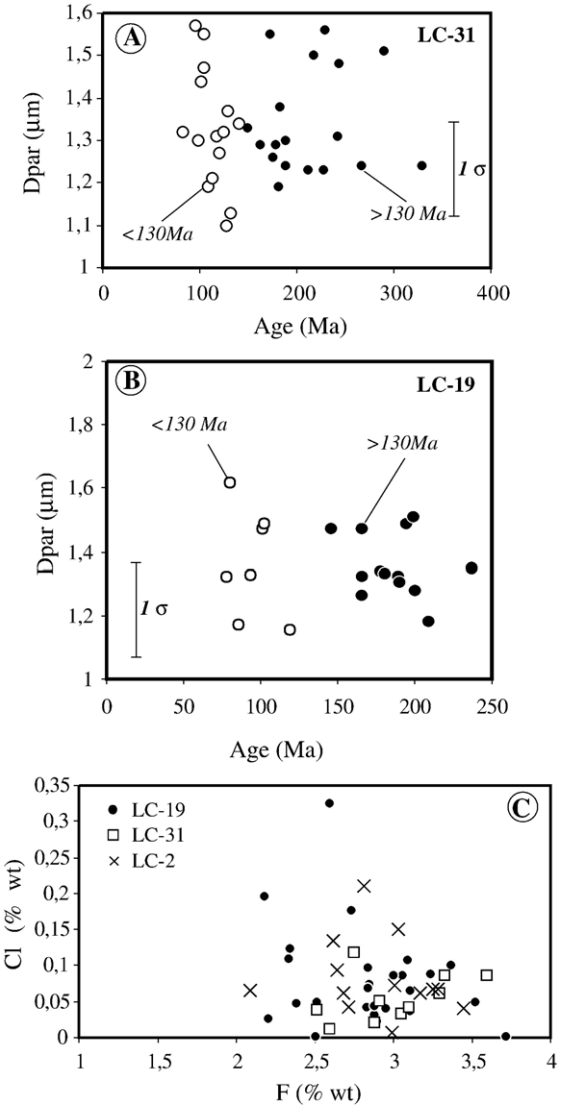

Fig. 5. A and B) D_{par} vs. apatite fission-track age in samples LC-19 and LC-31. Each D_{par} value in the diagram represents the average of four individual D_{par} measurements in a single grain. C) Cl vs. F contents in three Albian samples.

similar to Durango apatite. Modelling was performed using AFTSolve software by Ketcham et al. (2000). Geological constraints used for modelling included the depositional age and the timing of subsidence events in the Río Segura area (Hanne et al., 2003). Nevertheless, modelling proved to be robust also in the absence of the constraints related to the timing of subsidence events. In fact, Fig. 6 reveals that, apart from the constraints related to depositional time, the other constraints are set almost free and alternative models show similar T–t paths. This indicates that the results and interpretations are independent of the presence of subsidence-timing constraints.

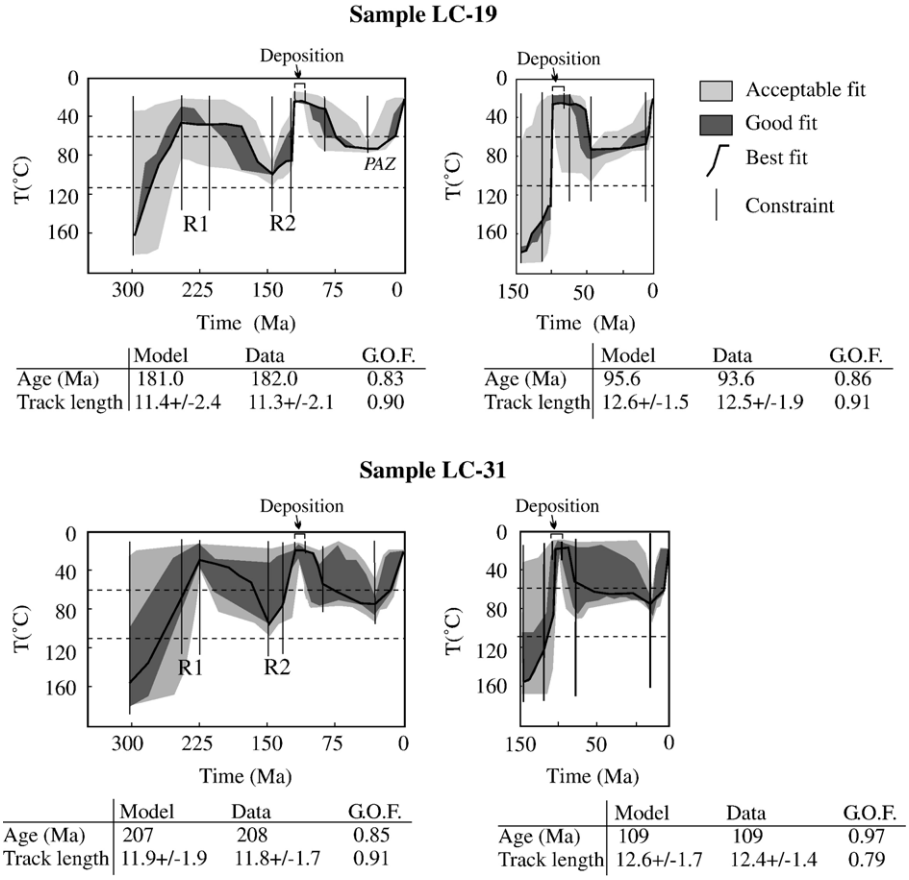

Fig. 6. Results of thermal modelling for the Lower Cretaceous samples LC-19 and LC-31 in which track lengths were assigned to their respective age population. Models were performed using AFTSolve software after Ketcham et al. (2000). G.O.F.=goodness of fit. R1, R2=intervals of the rifting processes as estimated by Hanne et al. (2003). Best model is indicated; dashed line indicates parts of the time–temperatures path unconstrained by modelling except for deposition time. Horizontal dashed lines are the upper and lower limits of the apatite fission-track annealing zone.

Modelled time–temperature paths of the younger population (Fig. 6) showed progressive heating since the Albian, maximum temperature not exceeding 70–80 °C, which is compatible with vitrinite reflectance Ro=0.5% data from Albian sediments in the Socovos-2 borehole located not far from the study area (Barbero et al., 2001). Models also indicate that the source rocks for the ~90–100 Ma population might have been rapidly exhumed just before deposition, thus having an very short pre-depo>sitional apatite fission-track thermal history that will very weakly influence the subsequent post-depositional track pattern. From modelling, it appears that sediments remained at temperatures of 70–80 °C for most of the Tertiary, the last cooling event shown by the models started at 15–20 Ma.

In the modelling of the thermal evolution of the source area (old-age component) the results of the post-depositional history of the younger populations were used as constraints, as after deposition both age components shared the same thermal evolution. Fig. 6 illustrates the results of the best fits for samples LC-19 and LC-31. The thermal evolution is characterized by a progressive cooling of the source area through the apatite partial-annealing zone during late Carboniferous to Permian times, followed by a progressive heating episode that finished at approximately 150 Ma at temperatures close to 90–100 °C. After this heating episode, a rapid cooling from maximum temperatures at 140 Ma to surface temperatures at 110 Ma is observed.

6. Discussion

6.1. Triassic thermal evolution

Triassic samples from the Tabular Cover are deposited directly on top of the Palaeozoic basement, a position that helps to establish the thermal evolution of the autochthonous Betic margin. Apatite fission-track results in these

samples indicated that during their post-depositional evolution maximum temperatures of 100–110 °C were reached. This clearly indicates that for the Triassic samples located at the Tabular Cover close to the Hercynian basement, significant apatite fission-track annealing occurred after Carnian–Ladinian times.

In the Triassic samples, the populations younger than the depositional age showed apatite fission-track ages close to the AFT ages of basement samples from the area (Stapel, 1999). The short mean track lengths (10.4 μm), although not enough to allow modelling, indicate that annealing must have occurred long after deposition, because long tracks are very scarce.

Source areas for the Triassic sandstones must be located in the Hercynian basement that was already cropping out in certain parts of the Iberian plate. Results from a transverse section through the southern limit of the Hercynian basement indicate that, in the West Iberian region, temperatures within the apatite PAZ cooled rapidly at 112 and 60 Ma, but in the Central Iberian Zone cooling appears to have very slowly crossed the apatite PAZ during Permo-Triassic times (Stapel, 1999) as is also the case of other parts of the Hercynian basement in the Central Iberian Zone (Barbero et al., 2005) (Fig. 7). Thus, source areas for the Triassic sediments must be located in the Central Iberian zone, to the west of the suture between the so-called Ossa Morena and Central Iberia zone.

The Triassic evolution is characterized by an initial Permo-Triassic cooling period of the source areas which occurred at rates of 10–13 °C/Ma, due to exhumation of the source areas, followed by a heating period which corresponds to the subsidence period proposed by Hanne et al. (2003). This is also observed when studying the thermal evolution of certain parts of the Hercynian basement such as the Montes de Toledo area, Central Hercynian zone (Barbero et al., 2005). The thermal evolution of the Hercynian crust during the Triassic could result from a combination of major thermomechanical processes such as (a) the relaxation of the thermal anomaly related to the end of the Hercynian cycle, (b) the progressive erosion of the Hercynian basement and (c) the thermal subsidence related to the rifting of the Bay of Biscay (Hanne et al., 2003; Barbero et al., 2005), the erosion factor being dominant.

6.2. Jurassic thermal evolution

Thermal models show that after the Permo-Triassic cooling episode a heating period commenced in Early Triassic times and ended at Tithonian times (152–145 Ma). This heating episode marks the final erosion-related cooling of the Hercynian crust and subsequent dominance of the subsidence related to the Jurassic rifting. The beginning of the Jurassic rifting is characterized by an intracontinental stage during which sedimentation changed from shallow towards more basinal environments. The presence of mantle-derived tholeiitic basalts interbedded within Upper Triassic sediments probably marked the initial stages of rifting (Morata, 1993; Molina et al., 1998; Vera, 2001). Also, the presence of anorogenic alkaline dykes of Triassic age in the Central Hercynian zone cut by the Messejana–Plasencia tholeiitic dyke, intruded between 203 and 184 (Shermerhorn et al., 1978; Dunn et al., 1998), also indicates active rifting related to the initial opening of the Atlantic ocean from Triassic to Jurassic times (Villaseca et al., 1992, 1999). This magmatism could also have

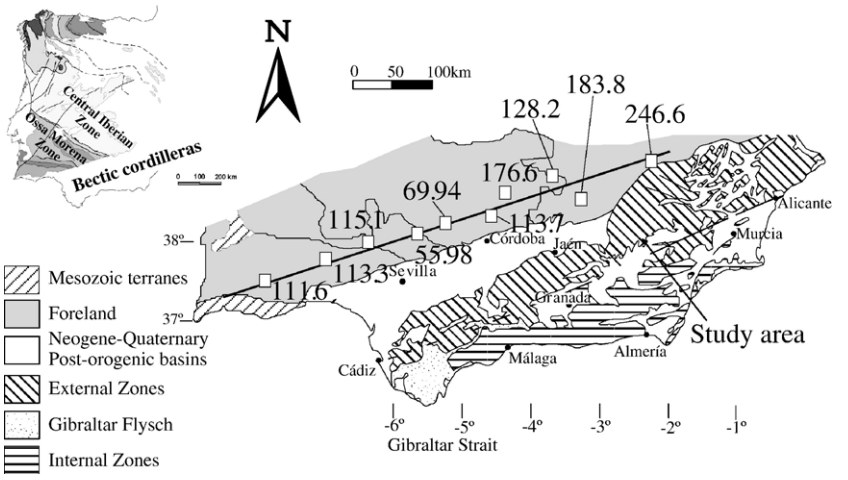

Fig. 7. Apatite fission-track ages in a traverse from the South Portuguese zone to Central Iberian zone from Stapel (1999). Inset shows the location of the Central Iberian and Ossa Morena Zones in the context of the Hercynian basement.

contributed to an increase of the geothermal gradient during rifting. Subsidence analysis performed by Hanne et al., 2003, in the Rio Segura section gave a total depth after Jurassic rifting of around 2000 m. When the application of a geothermal gradient typical of rifting scenarios with associated magmatism (~45 °C/km) to this depth deduced from the subsidence analysis, the predicted temperature (around 90 °C) is similar to those given by the fission-track modelling.

It is noteworthy that the Jurassic heating event is also visible in certain parts of the Hercynian basement (Barbero et al., 2005), which therefore evidences an evolution of plate scale and underlines the importance of the far-field effect during the rifting process.

6.3. Cretaceous thermal evolution

The source areas for the Aptian–Albian terrigenous sediments may be either the Triassic sandstones or the Hercynian basement. The Jurassic stratigraphy is completely dominated by carbonates, excluding them as potential source area. The presence of tourmaline, garnet, zircon, apatite, rutile, opaque minerals, and sillimanite in the heavy-mineral association, together with the quartz-rich character of the sediments, points to a provenance from peraluminous quarzofeldspatic igneous rocks or high-temperature metamorphic rocks, most probably from the Hercynian basement.

The end of the Triassic–Jurassic rifting is well marked by a cooling event probably starting during Neocomian times and ending at Cretaceous surface temperatures by the Albian. During the Late Jurassic to Early Cretaceous a graben–horst structure due to lithosphere stretching was created (Ziegler, 1990). One of the consequences of thermal doming is local uplift of the horst structures which could be subsequently eroded, thus leading to the Neocomian–Lower Cretaceous cooling event reflected in the thermal models. Thermal doming of the lithosphere occurred, the effects of which are particularly evidenced by the presence of continental to deltaic deposits (the Albian white sands and sandstones) in the eastern shelf facing the Sudiberian margin (Ziegler, 1990). This seems to be the case, on the basis of the sedimentological data (continental detrital deposits and shallow marine sedimentation typical of rift flanks rather than of typical basinal areas) and on the basis of the thermal models. Far-field effects of this thermal doming are also evidenced by cooling episodes registered in thermal models based on apatite fission-track data in areas located in the Iberian plate interior (Barbero et al., 2005).

Following this cooling a heating event is recognized in the thermal models throughout the Late Cretaceous. This heating is traditionally associated to subsidence and is particularly evident from the basins which surround the Iberian microplate where several authors established similar subsidence curves (Schwentke and Kuhnt, 1992; Gräfe and Wiedmann, 1993; Ziegler et al., 1995; Stapel et al., 1996; Martín-Chivelet et al., 1997). This subsidence was due largely to the convergence between the Iberian and the African plates, added to certain effect of the Bay of Biscay closing and the opening of the North Atlantic Ocean (Reicherter and Pletsch, 2000).

Subsidence rates deduced from the thermal models for the post-depositional evolution considering a geothermal gradient of 30 °C/km, which is normal in a passive margin like this, are around 60 m/Ma. These subsidence rates are similar to those calculated by Martín-Chivelet (1996) for the Yecla–Jumilla area in the External Betics (but further to the northeast) and are typical of a passive margin situation. The fact that the Aptian–Albian sediments represent shallow marine environments together with the fact that the maximum thickness of this facies is around 1000 m (in the proximity of Yeste, Fig. 1) confirm this continuous subsidence of the Betic margin from the Albian to the Mesozoic–Cenozoic limit.

7. Conclusions

Two different apatite-age components were distinguished in the Albian deposits of the Sierra de Segura region. The younger age component exhibits an apatite fission-track age which is younger but very close to the depositional age, thus indicating very little thermal disturbance since deposition. Thermal models confirm that the source area for the young age component in the Albian sediments must have been rapidly exhumed shortly before deposition. The post-depositional thermal history was then used to model the thermal history of the old age component found in the Albian sediments in this part of the External Betics.

The Triassic thermal evolution is characterized by an initial Permo-Triassic cooling, probably related to the end of the Hercynian cycle and its subsequent denudation. A subsequent heating is related to the subsidence due to initial phases of rifting in the Atlantic (Hanne et al., 2003). During the Jurassic, subsidence and temperature rise continues to be accompanied by extensive upper-crustal-level magmatism in the area (see Vera, 2001, for a compilation) which may have contributed to the total thermal budget. Heating finished at approximately 145–150 Ma and a period of rapid cooling is followed. This rapid cooling could be the consequence of thermal doming which led to cooling in the uplifted marginal rift areas

(Ziegler, 1990) and is supported by sedimentological data (continental detrital deposits, shallow marine sedimentation, etc.). Finally, during the Cretaceous and Cenozoic, there was a moderate temperature rise, which has traditionally been assigned to subsidence related to convergence between the Iberian and African plates. In the Miocene, a rapid cooling period was related to the extensional collapse of the Internal zone of the Betic orogen (Sosson et al., 1998) and therefore it is not considered to be an artefact of the thermal modelling algorithm.

Acknowledgements

Detailed comments made by Peter van der Beek, Istvan Dunkl, Meinert Rahn and Jurgen Foeken on a previous version of the manuscript are greatly appreciated. David Nesbitt is thanked for the revision of the English version of the text. This work has been financially supported by the project 1FD97-0732 co-financed by FEDER and the Ministerio de Ciencia y Tecnología and by Grupos de Investigación RNM 160 and RNM 163 of the PAI (Junta de Andalucía).

References

Arias, C., Masse, J.P., Vilas, L., 1996. Relaciones tectónica-sedimentación en el Aptiense de Sierra, Larga Jumilla (Murcia). Geogaceta 20, 43–46.

Banks, C.J., Warburton, J., 1991. Mid-crustal detachment in the Betic system of southeast Spain. Tectonophysics 191, 275–289.

Barbero, L., López-Garrido, J.A., García-Hernández, M., Quesada, S., Martínez del Olmo, W., 2001. Evolución termal Mesozoica de la Cuenca Prebética (Sierra de Segura) inferida mediante análisis de huellas de fisión en apatito: resultados preliminares. Geotemas 3 (2), 155–160.

Barbero, L., Glasmacher, U.A., Villaseca, C., López-García, J.A., Martín-Romera, C., 2005. Long-term thermo-tectonic evolution of the Montes de Toledo area (central Hercynian Belt): constraints from apatite fission track analysis. Int. J. Earth Sci. 94, 193–203.

Brandon, M.T., 1992. Decomposition of fission-track grain-age distributions. Am. J. Sci. 292, 535–564.

Brandon, M.T., 1996. Probability density plot for fission-track grain-age samples. Radiat. Meas. 26, 663–676.

Dabrio, J.C., López-Garrido, A.C., 1970. Estructura en escamas del sector noroccidental de la Sierra de Cazorla (Zona Prebética) y del borde de la Depresion del Guadalquivir (Prov. de Jaén). Cuad. Geol. - Univ. Granada 1, 149–157.

De Ruig, M.J., 1992. Tectono-sedimentary evolution of the Prebetic Fold Belt of Alicante (SE Spain). A study of stress fluctuations and foreland basins deformation. PhD Thesis, University of Amsterdam, 207 pp.

Dunkl, I., 2001. TRACKEY: a Windows program for calculation and graphical presentation of fission track data. Comput. Geosci. 28 (1), 3–12.

Dunn, A.M., Reynolds, P.H., Clarke, B., Ugidos, J.M., 1998. A comparison of the age and composition of the Shelbourne Dyke, Nova Scotia, and the Messejana Dyke, Spain. Can. J. Earth Sci. 35, 1110–1115.

Galbraith, R.F., Green, P.F., 1990. Estimating the component ages in a finite mixture. Nucl. Tracks Radiat. Meas. 17, 197–206.

Gallagher, K., 1995. Evolving temperature histories from apatite fission-track data. Earth Planet. Sci. Let. 136, 421–435.

Gallagher, K., Brown, R.W., 1997. The onshore record of passive margin evolution. J. Geol. Soc. (Lond.) 154, 451–457.

Gallagher, K., Brown, R.W., Johnson, C.J., 1998. Geological applications of fission track analysis. Annu. Rev. Earth Planet. Sci. 26, 519–572.

García-Hernández, M., López Garrido, A.C., Pulido Bosch, A., 1973. Observaciones sobre el contacto Subbético-Prebético en el sector de Nerpio. Cuad. Geol. - Univ. Granada 4, 77–91.

García-Hernández, M., González Donoso, J.M., Linares, A., Rivas, P., Vera, J.A., 1976. Características ambientales del Lías Inferior y medio en la Zona Subbética y su significado en la interpretación general de la cordillera. Reunión sobre la Geodinámica de la Cordillera Bética y Mar de Alborán. Sec. Pub. Univ. Granada, pp. 125–157.

García-Hernández, M., López-Garrido, A.C., Rivas, P., Sanz de Galdeano, C., Vera, J.A., 1980. Mesozoic palaeogeographic evolution of the External zone of the Betic Cordillera. Geol. Mijnb. 59, 155–168.

García-Hernández, M., López-Garrido, A.C., Vera, J.A., 2004. El prebético del sector central y afloramientos más occidentales. In: Vera, J.A. (Ed.), Geología de España. Sociedad Geológica de España-Instituto Geológico y Minero de España, Madrid, pp. 363–365.

Garver, J.I., Brandon, M.T., 1994. Erosional denudation of the British Columbia Coast Region as determined from fission-track ages of detrital zircon from the Tofiño Basin, Olympic Peninsula, Washington. Geol. Soc. Amer. Bull. 106, 1398–1412.

Gil, A., Fernández, J., López-Garrido, A.C., 1987. Evolución de facies en el Trías de la Zona Prebética y borde de la Meseta. Transversal Orcera-Puente Génave (Prov. Jaén). Cuad. Geol. Ibér. 11, 403–420.

Gräfe, K.-U., Wiedmann, J., 1993. Sequence stratigraphy in the Upper Cretaceous of the Basco–Cantabrian Basin (northern Spain). Geol. Rundsch. 82, 327–361.

Hanne, D., White, N., Lonergan, L., 2003. Subsidence analyses from the Betic Cordillera, southeast Spain. Basin Res. 15, 1–21.

Hurford, A.J., Green, P., 1983. The zeta calibration of fission-track dating. Chem. Geol., Isot. Geosci. Sect. 1, 285–317.

Ketcham, R.A., Donelick, R.A., Carlson, W.D., 2000. AFTSolve: a program for multi-kinetic modeling of apatite fission-track data. Geol. Mater. Res. 2, 1–32.

Laslett, G.M., Green, P.F., Duddy, I.R., Gleadow, A.W., 1987. Thermal annealing of fission-track in apatite. 2. A quantitative analysis. Chem. Geol., Isot. Geosci. Sect. 65, 1–13.

Lonergan, L., Johnson, C., 1998. Reconstructing orogenic exhumation histories using synorogenic detrital zircons and apatites: an example from the Betic Cordillera, SE Spain. Basin Res. 10, 353–364.

Martín-Chivelet, J., 1996. Late Cretaceous subsidence history of the Betic Continental Margin (Jumilla–Yecla region, SE Spain). Tectonophysics 265, 191–211.

Martín-Chivelet, J., Giménez, R., Luperto-Sinni, E., 1997. La discontinuidad Campaniense basal en el Prebético: ¿inicio de la convergencia alpina en la Margen Bética? Geogaceta 22, 121–124.

Martín-Chivelet, J., Berasategui, X., Rosales, I., Vilas, L., Vera, J.A., Caus, E., Gräfe, K.-U., Mas, R., Puig, C., Segura, M., Robles, S., Floquet, M., Quesada, S., Ruiz-Ortiz, P., Fregenal-Martínez, M.A., Salas, R., Arias, C., García, A., Martín-Algarra, A., Meléndez, N., Chacón, B., Molina, J.A., Sanz, J.L., Castro, J.M., García-Hernández, M., Carenas, B., García-Hidalgo, J., Gil, J., Ortega, F., 2002. Cretaceous. In: Gibbons, W., Moreno, T. (Eds.), The Geology of Spain. Geological Society, London, pp. 255–292.

Molina, J.M., Vera, J.A., De Gea, G., 1998. Vulcanismo submarino del santoniense en el subbético: datación con nannofósiles e interpretación

(Formación capas Rojas Alamedilla, provincia de Granada). Estud. Geol. 54, 191–197.

Morata, D., 1993. Petrología y geoquímica de las ofitas de las Zonas Externas de las Cordilleras Béticas. PhD thesis, Universidad de Granada, 342 pp.

Peper, T., Cloetingh, S., 1992. Lithosphere dynamics and tectono-stratigraphic evolution of the Mesozoic Betic rifted margin (southeastern Spain). Tectonophysics 203, 345–361.

Pérez-López, A., 1991. El Trías de facies germánica en el sector central de la Cordillera Bética. PhD Thesis, Universidad de Granada, 400 pp.

Reicherter, K.R., Pletsch, T.K., 2000. Evidence of a synchronous circum-Iberia subsidence event and its relation to the African–Iberian plate convergence in the Late Cretaceous. Terra Nova 12, 141–147.

Sanz de Galdeano, C., 1990. Geologic evolution of the Betic Cordilleras in the western Mediterranean Miocene to Present. Tectonophysics 172, 107–119.

Shermerhorn, L.J.G., Priem, H.N.A., Boelrijk, N.A.I., Hebeda, E.H., Verdumen, E.A.T., Vercluse, R.H., 1978. Age and origin of the Messejana dolerite fault dyke system (Portugal and Spain) in the light of the North Atlantic Ocean. J. Geol. 86, 229–309.

Schwentke, W., Kuhnt, W., 1992. Subsidence history and continental margin evolution of the western Pyrenean and Basque basins. Palaeogeogr., Palaeoclimatol., Palaeoecol. 95, 297–318.

Sosson, M., Morillon, A.C., Bourgois, J., Féraud, G., Poupeau, G.Y., Saint-Marc, P., 1998. Late exhumation stages of the Alpujárride Complex (western Betic Cordilleras, Spain): new thermochronological and structural data on Los Reales and Ojén nappes. Tectonophysics 285, 253–273.

Stapel, G., 1999. The Nature of isostasy in west Iberia and its bearing on Mesozoic and Cenozoic regional tectonics. PhD Thesis, Vrije Universiteit, 148 pp.

Stapel, G., Cloetingh, S., Pronk, B., 1996. Quantitative subsidence analysis of the Mesozoic evolution of the Lusitanian Basin. Tectonophysics 266, 493–507.

Vegas, R., Banda, R., 1982. Tectonic framework and Alpine evolution of the Iberian Peninsula. Earth Evol. Sci. 2 (4), 320–343.

Vera, J.A., 1981. Correlación entre las Cordilleras Béticas y otras cadenas alpinas durante el Mesozoico. Programa Internacional de Correlación Geológica (PICG), vol. 2. Real Academia de Ciencias Exactas, Físico-Químicas y Naturales, Madrid, pp. 125–160.

Vera, J.A., 1988. Evolución de los sistemas de depósitos en el margen ibérico de la Cordillera Bética. Rev. Soc. Geol. Esp. 1, 373–391.

Vera, J., 2001. Evolution of the south Iberian continental margin. In: Ziegler, P.A., Cavazza, W., Roberston, A.H.F., Crasquin-Soleau, S. (Eds.), Peri-Tethys Memoir 6: Peri-Tethyan Rift/Wrench Basins and Passive Margins. Mém. Mus. Natn. Hist. Nat., vol. 186, pp. 109–143.

Vera, J., Martín-Algarra, A., 2004. Cordilleras Béticas y Baleares. Divisiones mayores y nomenclatura. In: Vera, A. (Ed.), Geología de España. Sociedad Geológica de España-Instituto Geológico y Minero de España, Madrid, pp. 348–350.

Vilas, L., Dabrio, C., Peláez, J.R., García-Hernández, M., 2001. Dominios sedimentarios generados durante el periodo extensional Cretácico Inferior entre Cazorla y Hellín (Béticas Externas). Su implicación en la estructural actual. Rev. Soc. Geol. Esp. 14, 113–122.

Villaseca, C., Huertas, M.J., Nuez, J., 1992. Magmatismo postorogénico y anorogénico en el Sistema Central Español. Geogaceta 11, 34–37.

Villaseca, C., Downes, H., Pin, C., Barbero, L., 1999. Nature and composition of the lower continental crust in central Spain: inferences from granulitic xenoliths and implications on the granulite–granite linkage. J. Petrol. 40, 1465–1496.

White, N.J., 1993. Recovery of strain rate variation from inversion of subsidence data. Lett. Nat. 366, 449–452.

Ziegler, P., 1990. Geological Atlas of western and central Europe. Shell Internationale Petroleoum Maatsschappij. 239 pp.

Ziegler, P.A., Cloetingh, S., Van Wees, J.-D., 1995. Dynamics of intra-plate compressional deformation: the Alpine foreland and other examples. Tectonophysics 252, 7–59.